

GalevNB: a conversion from N-BODY simulations to observations

Xiaoying Pang^{1,2,5}, Christoph Olczak^{1,3}, Difeng Guo^{1,3}, Rainer Spurzem^{1,4,3,6} and Ralf Kotulla⁷

¹ National Astronomical Observatories and Key Laboratory of Computational Astrophysics, Chinese Academy of Sciences, 20A Datun Road, Chaoyang District, 100012 Beijing, P.R. China;
xypan@bao.ac.cn

² Shanghai Institute of Technology, 100 Haiquan Road, Fengxian district, Shanghai 201418, P.R. China

³ Astronomisches Rechen-Institut, Zentrum für Astronomie der Universität Heidelberg, Mönchhofstr. 12–14, 69120 Heidelberg, Germany

⁴ Kavli Institute for Astronomy & Astrophysics, Peking University, 5 Yi He Yuan Road, Hai Dian District, Beijing 100871, P.R. China

⁵ Key Lab for Astrophysics, Shanghai Normal University, 100 Guilin Road, Shanghai 200234, P.R. China

⁶ Key Laboratory of Frontiers in Theoretical Physics, Institute of Theoretical Physics, Chinese Academy of Sciences, Beijing, 100190, P.R. China

⁷ Department of Astronomy, University of Wisconsin - Madison, 475 N Charter St, Madison WI 53706, USA

Abstract We present GalevNB (Galev for N -body simulations), an utility that converts fundamental stellar properties of N -body simulations into observational properties using the GALEV (GALaxy EVolutionary synthesis models) package, and thus allowing direct comparisons between observations and N -body simulations. It works by converting fundamental stellar properties, such as stellar mass, temperature, luminosity and metallicity into observational magnitudes for a variety of filters of mainstream instruments/telescopes, such as HST, ESO, SDSS, 2MASS, etc.), and into spectra that spans from far-UV (90 Å) to near-IR (160 μ m). As an application, we use GalevNB to investigate the secular evolution of spectral energy distribution (SED) and color-magnitude diagram (CMD) of a simulated star cluster over a few hundred million years. With the results given by GalevNB we discover an UV-excess in the SED of the cluster over the whole simulation time. We also identify four candidates that contribute to the FUV peak, core helium burning stars, thermal pulsing asymptotic giant branch (TPAGB) stars, white dwarfs and naked helium stars.

Key words: stars: kinematics and dynamics—stars: C-M diagrams—stars: AGB and post-AGB —stars:white dwarf

1 INTRODUCTION

Models of dense stellar systems, such as globular or young dense stellar clusters, or nuclear star clusters with or without massive central black hole, require direct N -body simulations, which at least resolve and follow all stellar orbits in a star cluster as precisely as possible given the usable hardware and computing time. But due to the strong dependence on initial conditions of the gravitational N -body problem, which originates from close encounters, the system is physically and numerically unstable (Miller

1966). Therefore results of direct high-accuracy N -body simulations should always be carefully analyzed, as they represent individual realizations of physically possible solutions. In another word, small variations of initial conditions may lead to different results with regard to individual objects or events. Nevertheless, the coarse-grained evolution (densities, distribution functions) is quite well following expectations from statistical mechanics (see e.g. Giersz & Spurzem 1994, Spurzem & Aarseth 1996). And the simulations are an excellent tool to examine and study physical processes in star clusters.

The sequence of high-accuracy direct N -body codes developed by Sverre Aarseth (Aarseth 1999; Aarseth 2003) is among the most widely used if not *the* most widely used code. Its most notable features are the Hermite 4th order integration scheme, the hierarchically blocked individual time steps (Makino & Aarseth 1992), the Kustaanheimo-Stiefel (KS) regularization for strong interactions (Kustaanheimo & Stiefel 1965) and its generalizations for few-body subsystems (chain regularization, Mikkola & Aarseth 1993), and the Ahmad-Cohen neighbor scheme (Ahmad & Cohen 1973). NBODY6++ is the current massively parallel version of NBODY6 (Spurzem 1999, Spurzem et al. 2008), and NBODY6++GPU adds to it the use of accelerating many-core hardware (GPU) on every node (Wang et al. 2015). In the cited paper it becomes clear that direct N -body simulations with a million particles are feasible now. The challenges of the resulting massive simulation data and their possible approaches of management are addressed in Cai et al. (2014).

However, the output parameters of N-BODY simulations are mostly theoretical values. To make a direct comparison between our simulation data and observations, we combine GALEV (GALaxy EVolutionary synthesis models; Kotulla et al. 2009), a flexible algorithm to combine astrophysical colors in many filters and spectra of stars (Lejeune, Cuisinier & Buser 1997, 1998) or sets of stars, with NBODY6++GPU simulations. In this paper, we present this new code: GalevNB (Galev for N -body simulation) and its application in NBODY6++GPU simulation data. Adapting subroutines from GALEV, GalevNB can produce spectra spans the range from far-UV (FUV) at 90 Å to far IR at 160 μ m, with a spectral resolution of 20 Å in the UV-optical and 50-100 Å in the near IR range. Given a list of requested filters in HST, ESO, SDSS, 2MASS etc., GalevNB convolves the spectra with the filter response functions and applies the chosen zero-points (Vegamag, ABmag, and STmag) to yield absolute magnitudes. GalevNB bridges theoretical parameters and their observed values, thus allows us to understand the color and spectra evolution of star clusters, and to determine the initial conditions and parameters of star cluster simulations with a direct comparison to observations.

Though most Galactic and many Local Group clusters are resolved, observing individual stars in extragalactic star clusters is extremely challenging due to severe crowding. Therefore, integrated photometry and spectroscopy have been used to identify extragalactic star clusters and obtain parameters (Bica et al. 1996a, Sarajedini et al. 2007, Peng et al. 2008, 2009, Johnson et al. 2012), and even to investigate multiple stellar populations (Peacock et al. 2013). Using the imaging obtained with the High Resolution Channel of the Advanced Camera for Surveys on board HST, Larsen et al. (2011) manage to construct color magnitude diagrams (CMDs) for several extragalactic star clusters within 5 Mpc. However, for the very distant star clusters, such as the ones in Antennae galaxies (~ 22 Mpc, Whitmore et al. 2007, Bastian et al. 2009), or in Virgo cluster (~ 16.5 Mpc, Peng et al. 2008, Peng et al. 2009), studies of individual stars are still not possible. Integrated colors can be used to derive the age of star clusters generally (Elson & Fall 1985). However, metal variation, stochastic effect (Girardi et al. 1995), and dynamical evolution (Fleck et al. 2006) will change integrated colors. Therefore, integrated photometry may not be enough to decouple the stellar and dynamical effects of distant star clusters. With GalevNB producing observational magnitudes and spectra for N -BODY simulations, it allows us to investigate stellar evolution and dynamics (via colors and spectra) in distant star clusters at the same time, and even make prediction for observations.

In this paper, we carry out star cluster simulations with NBODY6++GPU codes, and use GalevNB to produce observational data for the simulated cluster. The computational methods of NBODY6++GPU simulations are summarized in Section 2. An introduction to the structure and execution procedure of GalevNB is presented in Section 3. The observational features of the simulated cluster, CMDs and spectral energy distributions (SEDs) are outlined in Section 4. Finally, we present our discussion and summary in Section 5.

2 COMPUTATIONAL METHOD AND INITIAL CONDITIONS

The model clusters in this work are evolved using NBODY6++GPU which is the MPI parallel version based on the state-of-the-art direct N -body integrator NBODY6GPU (Aarseth 2003, Nitadori & Aarseth 2012). Gravitational forces are computed using a fourth-order Hermite integration scheme with block time steps (and without softening). The code includes algorithms for stellar and binary evolution (Tout et al. 1997, Hurley et al. 2000) and deals directly with perturbations to binary orbits, collisions and mergers, formation of three- and four-body subsystems, exchange interactions and tidal capture. The treatment of close encounters constitutes a large part of the code.

We set up a simple dynamical model of a massive stellar cluster, as an example for GalevNB to work on. The stellar system is initially gas-free, and is assumed in virial equilibrium as an approximation after losing gas (i.e. the ratio of kinetic to potential energy is $Q_{\text{vir}} = 0.5$). The single-aged population is run with $N_0 = 10\,000$ single stars. Million-particle simulations of star clusters will be shown in our coming paper. The IMF is set up according to Kroupa (2001) with fixed lower and upper mass limits, $m_l = 0.1 M_\odot$ and $m_u = 20 M_\odot$, respectively, resulting in an initial cluster mass of $M_0 = 4.7 \times 10^3 M_\odot$. To simplify the computation, stars are distributed according to Plummer model with a scale radius of 0.59 pc, which does not differ significantly from King model with $W_0 = 6$, except in the outermost regions with low density. The models have an initial half-mass radius $R_{\text{hm}} = 0.76$ pc, and is not primordially mass segregated. We set the metallicity to sub-solar metallicity $Z_\odot = 0.001$, which is similar to the halo population of Galactic globular clusters. Note that our simulated star cluster is still less massive than a typical Galactic globular cluster. But here we are interested in special spectral features, such as the production of UV bright stars, and aim to relate the current simulations to future million particle simulations.

Since our primary interest is the short-term stellar evolution, we therefore carry out a simulation of 3000 N -body time units (corresponding to 655.6 Myr) with dynamical and internal stellar evolution. Snapshots of the simulation are selected to display in this paper for the presence of UV-bright stars (see Section 4).

3 GALEVNB: GALEV FOR N -BODY SIMULATIONS

3.1 GalevNB Structure

In this section, we introduce the GalevNB structure and its parameters. The main program of GalevNB is `GalevNB.f90`, which parses single snapshot files (stellar evolution only) generated by NBODY6++GPU (NBODY6++)/ NBODY6GPU (NBODY6). It invokes seven subroutines (`startomaginit`, `specint_initialize`, `reset_weights`, `startomag`, `add_star`, `spec2mag`, `spec_output`) of GALEV package to convert effective temperature, stellar luminosity, metallicity, and mass into observational magnitudes and spectra. The functions of these routines are presented in Table 1. The GalevNB package contains four folders: 1) `spectral_templates`, in which all the spectral template files from the BaSeL library of model atmospheres (Lejeune, Cuisinier & Buser 1997, 1998) are stored; 2) `standard_filters`, containing a large set of filter response functions (FUV, NUV, U, B, V, R, I, J, H, K) that are used as standard reference filters; 3) `filter_response_curves`, including filter response functions from magnitude systems of HST, ESO instruments, 2MASS, SDSS, Johnson, and Cousins in separate subfolders. We also provide a choice of user-specify filter response functions. Information about the entire set of available filters is presented in the file `filterlist.dat`. Please aware that `filterlist.dat`, in which the user specify their own choice of magnitude system by uncommenting the row of chosen filter, MUST be presented in the same directory as the NBODY6++GPU (NBODY6++)/ NBODY6GPU (NBODY6) snapshot files. The content of the file, `filterlist.dat`, is presented in Table 2.

3.2 Installation and Usage of GalevNB

To compile GalevNB, the user should have C++ and fortran installed. The input file of GalevNB should be a single snapshot output from NBODY6++GPU (NBODY6++)/ NBODY6GPU (NBODY6) simulations. In case of

Table 1 Functions of subroutines converting theoretical parameters into observational magnitudes and spectra

Subroutine	Function
<code>specint_initialize</code>	initialize the stellar spectra
<code>reset_weights</code>	reset the weight of stellar spectra
<code>add_star</code>	integrate the flux of all stars in the cluster
<code>spec_output</code>	output spectra
<code>startomaginit</code>	initialize the stellar magnitude
<code>spec2mag</code>	convolve the stellar spectra with the filter response function
<code>startomag</code>	compute magnitudes for stars

Table 2 Column contents for the filter information file: `filterlist.dat`

Column	Content	ID of zero point
1	Filter name	
2	Corresponding path of the filter response function	
3	ID of selected zero point (default value is 1)	
4	Standard zero point in the Vega magnitude system	1
5	Standard zero point in the AB magnitude system	2
6	Standard zero point in the ST magnitude system	3
7	Optional user-defined zero point	4

a file containing all snapshots (called `sev.83` in `NBODY6++GPU` / `NBODY6++` and `fort.83` in `NBODY6GPU` / `NBODY6`), we provide the user with a shell script `generate_snapshots.sh` in the folder, `scripts`, for retrieving single snapshot data out of `sev.83` and `fort.83`. The user can select his/her preferred filters (maximum 20) by uncommenting the row of the corresponding filter in `filterlist.dat`, and choose his/her desired magnitude system (Table 2). Magnitudes of individual stars and the whole cluster, and spectra of the cluster or chosen stellar types are produced, respectively. The code of `GalevNB` is published online¹. Users can download it through internet. We also provide examples of output files from `NBODY6++GPU` and `GalevNB` on the web².

4 OBSERVATIONAL FEATURES OF SIMULATED STAR CLUSTERS

With `NBODY6++GPU` simulations done in Section 2, and the computation of `GalevNB`, we are able to investigate early evolution of CMD and SED of a stellar population in a real dynamical environment. The output of `NBODY6++GPU` simulations contain integers to represent stellar type information (Hurley et al. 2000) of each individual stars (Table 3). This allows one to identify exotic objects in the star cluster based on the evolution of CMD and SED. It is true that cluster dynamics, such as close stellar encounters or the formation of binaries, can significantly alter the stellar populations in dense stellar systems (Djorgovski & Piotto 1993). Nevertheless, to simplify the `NBODY6++GPU` simulations that `GalevNB` works on, we do not consider primordial binaries in the current simulations. Therefore, stellar type 19-22 (binaries) do not present in our simulations. Due to the faintness of stellar remnant, stellar types 13-15 (though appear in our examples) are not included in the studies of CMD and SED.

4.1 SED & CMD evolution

After integrating fluxes of individual stars, `GalevNB` output total SED of the star cluster. In the main program, `GalevNB.f90`, user can choose to output SED of certain stellar types. Therefore, specific stars' contribution to the total SED of the cluster can be quantified. In Figures 1, 3, 5, 7, we display SEDs of

¹ <http://silkroad.bao.ac.cn/repos/galevnb>

² <http://silkroad.bao.ac.cn/~xiaoying/>

Table 3 Stellar type defined in the NBODY6++GPU codes

Integer	Stellar type
0	main sequence (MS) stars with $\text{mass} \leq 0.7 M_{\odot}$
1	MS with $\text{mass} \geq 0.7 M_{\odot}$
2	Hertzsprung Gap
3	Red Giant
4	Core Helium Burning
5	First (early) Asymptotic Giant Branch
6	Second Asymptotic Giant Branch (\sim Thermal Pulsing AGB)
7	Naked Helium Star MS
8	Naked Helium Star Hertzsprung Gap
9	Naked Helium Star Giant Branch
10	Helium white dwarf
11	Carbon/Oxygen White Dwarf
12	Oxygen/Neon White Dwarf
13	Neutron Star
14	Black Hole
15	Massless supernova remnant
19	Circularizing binary (c.m. value)
20	Circularized binary
21	First Roche stage (inactive)
22	Second Roche stage

the cluster (black line), of asymptotic giant branch (AGB) stars (red line), of naked Helium stars (green line), of white dwarfs (blue), and of core helium burning stars (cyan line) at different ages. Movies of the evolution of SED and CMD are available in the weblink provided in Section 3.2².

At very early age, massive stars first exhaust their hydrogen in the core and ignite core helium burning. These core helium burning stars are UV-bright (Figure 1) and very blue (Figure 2), which are also termed as blue loops (Stothers & Chin 1991, El Eid 1995). The UV peak in the SED of the cluster ($< 1000 \text{ \AA}$) is mainly due to the presence of these stars (Figure 1).

As the cluster evolves, the intensity of the UV-excess drops (Figure 3, 5, 7). Besides core helium burning stars, we find another three stellar types producing UV radiation, second AGB stars, white dwarfs, and naked helium stars.

1) Early AGB stars (stellar type = 5) are very red, and therefore mainly radiate in the red filters (Girardi 2000, Marigo et al. 2008, Salaris et al. 2014). After the third dredge-up, helium shells flash repeats many times. At this stage, early AGB becomes thermal pulsing AGB (TPAGB; Marigo et al. 2008, Hurley et al. 2000). In the NBODY6++GPU code, the TPAGB are called "second AGB" (stellar type = 6). The radii of the TPAGB grow so large that mass-loss is significant. At this time, the TPAGB reach very high temperature ($> 10^4 \text{ K}$) and begin to be luminous in the UV filters (Figure 3). Mass-loss will eventually remove all the envelopes of the TPAGB, which may be seen as planetary nebulae (see the CMD in Figure 4).

2) White dwarfs are born after the TPAGB turning into planetary nebulae. Though white dwarfs cool down eventually (Mestel 1952, Liebert 1980, Hansen & Liebert 2003), young white dwarfs are very hot and blue (Mestel 1952, Rauch et al. 2014, Torres et al. 2014), whose radiation is largely at the UV ($< 2000 \text{ \AA}$, Figures 5 & 7). Even though their luminosity at the UV is not high, their contribution to the UV-excess of the cluster is long-term and might not be neglected, since stars evolve to white dwarfs continually.

3) One short term radiator at the UV is the naked helium star, with extremely blue color over the main-sequence turn-off (Figures 7 & 8). They are massive stars losing hydrogen envelopes, the so-called Wolf-Rayet stars in observations (Crowther 2007, Shara et al. 2013). Since naked helium stars only appear at young age for a short time-scale, they cannot influence the UV-excess of the cluster in the long run.

5 DISCUSSION

We present an integrated software solution, GaLevNB, a translator that bridges NBODY (6++ / 6) simulations (with or without GPU) and observations. We run a short-term dynamical model of a star cluster based on NBODY6++GPU code, producing data for GaLevNB. GaLevNB computes observational magnitudes and spectra of stars by theoretical parameters, stellar mass, temperature, luminosity and metallicity, which are generated by NBODY6++GPU simulations. In the SED evolution of the simulated cluster, we found a UV-excess in the wavelength shorter than 2000 Å.

Similar phenomenon is found in elliptical galaxies and early-type spiral bulges whose SEDs surprisingly increase to shorter wavelengths over the range 2000 to 1200 Å, (Code 1969, Code et al. 1972, Faber 1983, Burstein et al. 1988, Kurucz 1991), in contrary to the expectation of an old stellar systems that are usually assumed to be dark in the FUV. This rise in the spectrum at wavelengths shorter than 2000 Å is called "UV upturn" or "UV-excess". The UV-excess resembles the Rayleigh-Jeans tail of a thermal source with effective temperature larger than 20000 K (Hills 1971). During the last decades, many efforts have been made to find out "culprits" of the UV-excess. In contrast to our simulated cluster whose age is young (up to 655.6 Myr), in most of the early-type galaxies young massive stars are absent (O'Connell 1986, Welch 1982, Buzzoni et al. 2012). Therefore, old, hot, low-mass stars become a more popular choice. Extreme blue horizontal branch stars, with core helium burning and very thin envelopes, might be promising for explaining this phenomenon. These stars are found in both metal-rich and metal-poor star clusters (Rich et al. 1997, Ferraro 1998, Li et al. 2013, Buzzoni et al. 2012), which makes their origins somehow ambiguous. Theorists proposed another candidate producing a significant amount of UV radiation, post-AGB stars (Buzzoni & Gonzalez-Lopezlira 2008), a quarter of which undergo TPAGB phase (Lawlor & MacDonald 2006). Some studies suggested that new-born white dwarfs were hot enough to emit moderate amount of UV photons (Hills 1971, Bica et al. 1996b). Recently, based on detail computations of binaries, Han et al. (2007) conclude that the brown dwarf binary should be a more promising candidate accounting for the UV-excess.

Most of the candidate stars mentioned above originate in the cluster environment. With the application of GaLevNB to NBODY6++GPU simulation data, we are able to observe the SED evolution of different stellar types. Through this way, we find out four kinds of hot, blue stars that are dominant in the UV-excess: core helium burning stars, second AGB (TPAGB), white dwarfs and naked helium stars. Among them, second AGB is a favorable candidate from theoretical point of view (O'Connell 1999). On the contrary, white dwarf's candidate position is controversial (Magris & Bruzual 1993, Landsman et al. 1998) because of low luminosity. The life time of naked helium stars is very short. Though they are very bright at the UV, their short-term emission makes them insignificant candidates. However, how the UV radiation of the candidate stars evolve in the long-term is beyond the scope of this paper, which cannot be achieved with a simple stellar model. A detailed NBODY6++GPU simulation investigating the evolution of UV-excess in star clusters, with more particles, realistic initial condition and primordial binaries, will be presented in our coming paper (Pang et al. in prep.). The NBODY6++GPU code in its latest GPU accelerated version is publicly available in Wang et al. 2015. We provide our scripts and subroutines of GaLevNB online¹. Please notice that these are compatible with both NBODY6++ & 6 (with or without GPU) version. Users of the other version of NBODY may have to adjust some data formats.

For more than a decade "simulating observations of simulations" has been a topic in the community of MODEST (MODElling Dense Star Clusters, see www.manybody.org/modest/ and Kouwenhoven et al. 2004). Hurley et al. (2005) have published a pioneering study, which presented a full Hertzsprung-Russell diagram (luminosity vs. effective temperature) of all stars in the cluster M67 obtained from a direct N -body simulation with NBODY6, to be directly comparable to observations. These capabilities come with the standard public versions of NBODY6 and NBODY6++ (with or without GPU) already. The Monte Carlo code MOCCA is now also providing similar capabilities (Giersz, Heggie & Hurley 2008); recently it has been extended to allow simulated observations of star clusters with specific telescopes using their colour windows and standard software used by observers (Askar et al. 2015). This work has been driven by future key observational projects (for example by Hubble Space Telescope) for globular clusters (e.g. Milone et al. 2014); however, to fully uncover the 6D dynamical structure and the 3D

gravitational potential, as well as the population history of star clusters, pure photometry may not be sufficient. Future deep high resolutions spectroscopic and spectrophotometric observations of globular and other star clusters are required in order to uncover one more dimension in velocity (radial velocity) and obtain more information about the stellar population through full spectra. Kacharov et al. (2014) and den Brok et al. (2014) provide examples on how kinematic data provide key insights into the dynamics of globular clusters (rotation and the quest for intermediate mass black holes). See also for an overview van de Ven (2010). Here the combination of the GALEV codes, previously mainly used for synthesis of galactic stellar populations (Kotulla et al. 2009) with our most recent direct N -body code for star clusters is a pioneering step to provide the corresponding full spectral information at any time and any region in the cluster, star-by-star or in integrated fields from the models.

Acknowledgements This work is funded by National Natural Science Foundation of China, No: 11443001 (XYP) and 11073025 (RS). XYP extends gratitude to the funds of National Natural Science Foundation of China, No: 11503015, and of Shanghai education committee, No: 1021ZK151009027-ZZyy15104, and of the talents introduction project of Shanghai Institute of Technology, No: 10120K156031-YJ2014-05. XYP and RS are members of the Silk Road Project Team in National Astronomical Observatories of China (NAOC, <http://silkroad.bao.ac.cn>), and acknowledge the technical support from this team. CO appreciates funding by the German Research Foundation (DFG) grant OL 350/1-1; CO and RS have been partly supported through computational resources of SFB 881 The Milky Way System (subproject Z2) at the University of Heidelberg, Germany, in particular the Milky Way supercomputer hosted and co-funded by the Jülich Supercomputing Center (JSC). XYP appreciates the travel grants of the DFG grant OL 350/1-1.

RS is grateful to support by the Chinese Academy of Sciences Visiting Professorship for Senior International Scientists, Grant Number 2009S1-5, and through the "Qianren" special foreign experts program of China, both at NAOC. The special GPU accelerated supercomputer laohu at the Center of Information and Computing at National Astronomical Observatories, Chinese Academy of Sciences, funded by Ministry of Finance of Peoples Republic of China under the grant ZDY Z2008-2, has been used for simulations, as well as smaller GPU clusters titan, hydra and kepler, funded under the grants I/80041-043 and I/84678/84680 of the Volkswagen Foundation at ARI/ZAH, University of Heidelberg, Germany.

R.K. gratefully acknowledges Financial support from the National Science Foundation under Grant No. 1412449, as well as from STScI theory grant HST-AR-12840.01-A.

We appreciate Dr. Peter Anders for promoting and coordinating the collaborations between our N -body team and the GALEV team. Our gratitude also to Long Wang and Maxwell Xu Cai for discussion and support in running simulations and programming. We also acknowledge Prof. Dr. Richard de Grijs from Peking University and Prof. Dr. Zhongmu Li from Dali University for helpful discussion during this work.

References

- Aarseth, S. J. 2003, *Gravitational N-body Simulations*, by Sverre J. Aarseth, pp. 430. ISBN 0521432723. Cambridge, UK: Cambridge University Press, November 2003
- Aarseth, S. J. 1999, *PASP*, 111, 1333
- Ahmad, A., & Cohen, L. 1973, *Journal of Computational Physics*, 12, 389
- Askar, A., Giersz, M., Pych, W., Olech, A., & Hypki, A. 2014, arXiv:1501.00417
- Bastian, N., Tranco, G., Konstantopoulos, I. S., & Miller, B. W. 2009, *ApJ*, 701, 607
- Bica, E., Claria, J. J., Dottori, H., Santos, J. F. C., Jr., & Piatti, A. E. 1996a, *ApJS*, 102, 57
- Bica, E., Bonatto, C., Pastoriza, M. G., & Alloin, D. 1996b, *A&A*, 313, 405
- Burstein D., Bertola F., Buson L. M., Faber S. M. Lauer T. R. 1988, *ApJ*, 328, 440
- Buzzoni, A., & González-Lópezlira, R. A. 2008, *ApJ*, 686, 1007
- Buzzoni, A., Bertone, E., Carraro, G., & Buson, L. 2012, *ApJ*, 749, 35

- Cai M. X. et al, 2015, ApJ Supplement accepted, <http://arxiv.org/abs/1506.07591>
- Code A. D. 1969, PASP, 81, 475
- Code A. D., Welch G. A. 1972, In Scientific Results from the Orbiting Astronomical Observatory, ed. Code A. D. (NASA SP-310), 559
- Crowther, P. A. 2007, ARA&A, 45, 177
- den Brok, M., van de Ven, G., van den Bosch, R., & Watkins, L. 2014, MNRAS, 438, 487
- Djorgovski, S., & Piotto, G. 1993, Structure and Dynamics of Globular Clusters, 50, 203
- El Eid, M. F. 1995, MNRAS, 275, 983
- Elson, R. A. W., & Fall, S. M. 1985, ApJ, 299, 211
- Faber S. M. 1983, Highlights of Astronomy, 6, 165
- Ferraro, F. R., Paltrinieri, B., Fusi Pecci, F., Rood, R. T., & Dorman, B. 1998, ApJ, 500, 311
- Fleck, J.-J., Boily, C. M., Lançon, A., & Deiters, S. 2006, MNRAS, 369, 1392
- Giersz, M., Heggie, D. C., & Hurley, J. R. 2008, MNRAS, 388, 429
- Giersz, M., & Spurzem, R. 1994, MNRAS, 269, 241
- Girardi, L. 2000, Massive Stellar Clusters, 211, 133
- Girardi, L., Chiosi, C., Bertelli, G., & Bressan, A. 1995, A&A, 298, 87
- Han, Z., Podsiadlowski, P., & Lynas-Gray, A.E. 2007, MNRAS, 380, 1098
- Hansen, B. M. S., & Liebert, J. 2003, ARA&A, 41, 465
- Hills J. G. 1971, A&A, 12, 1
- Hurley, J. R., Pols, O. R., Aarseth, S. J., & Tout, C. A. 2005, MNRAS, 363, 293
- Hurley, J. R., Pols, O. R., & Tout, C. A. 2000, MNRAS, 315, 543
- Johnson, L. C., Seth, A. C., Dalcanton, J. J., et al. 2012, ApJ, 752, 95
- Kacharov, N., Bianchini, P., Koch, A., et al. 2014, A&A, 567, A69
- Kotulla, R., Fritze, U., Weilbacher, P., & Anders, P. 2009, MNRAS, 396, 462
- Kouwenhoven, T., Portegies Zwart, S., Gualandris, A., et al. 2004, Astronomische Nachrichten Supplement, 325, 101
- Kroupa, P. 2001, MNRAS, 322, 231
- Kustaanheimo and E. Stiefel, Perturbation theory of Kepler motion based on spinor regularization, J. Reine Angew. Math., 1965, 218, 204
- Kurucz, R. L. 1991, Precision Photometry: Astrophysics of the Galaxy, 27
- Landsman, W., Bohlin, R. C., Neff, S. G., et al. 1998, AJ, 116, 789
- Larsen, S. S., de Mink, S. E., Eldridge, J. J., et al. 2011, A&A, 532, A147
- Lawlor, T. M., & MacDonald, J. 2006, MNRAS, 371, 263
- Lejeune, T., Cuisinier, F., & Buser, R. 1997, A&AS, 125, 229
- Lejeune, T., Cuisinier, F., & Buser, R. 1998, A&AS, 130, 65
- Li, C., de Grijs, R., Deng, L., & Liu, X. 2013, ApJ, 770, LL7
- Liebert, J. 1980, ARA&A, 18, 363
- Magris G., Bruzual G. 1993, ApJ, 417, 102
- Marigo, P., Girardi, L., Bressan, A., et al. 2008, A&A, 482, 883
- Makino, J., & Aarseth, S. J. 1992, PASJ, 44, 141
- Mestel, L. 1952, MNRAS, 112, 583
- Meiron, Y., Li, B., Holley-Bockelmann, K., & Spurzem, R. 2014, ApJ, 792, 98
- Mikkola, S., & Aarseth, S. J. 1993, Celestial Mechanics and Dynamical Astronomy, 57, 439
- Miller, R. H. 1966, The Theory of Orbits in the Solar System and in Stellar Systems, 25, 137
- Milone, A. P., Marino, A. F., Bedin, L. R., et al. 2014, MNRAS, 439, 1588

- Nitadori, K., & Aarseth, S. J. 2012, MNRAS, 424, 545
- O’Connell, R. W. 1999, ARA&A, 37, 603
- O’Connell, R.W., Thuan, T.X., & Puschell, J.J. 1986, ApJ, 303, L37
- Peacock, M. B., Zepf, S. E., & Finzell, T. 2013, ApJ, 769, 126
- Peng, E. W., Jordán, A., Blakeslee, J. P., et al. 2009, ApJ, 703, 42
- Peng, E. W., Jordán, A., Côté, P., et al. 2008, ApJ, 681, 197
- Rauch, T., Werner, K., Quinet, P., & Kruk, J. W. 2014, A&A, 566, AA10
- Rich, R. M., Sosin, C., Djorgovski, S. G., et al. 1997, ApJ, 484, L25
- Salaris, M., Weiss, A., Cassarà, L. P., Piovan, L., & Chiosi, C. 2014, A&A, 565, AA9
- Sarajedini, A., Barker, M. K., Geisler, D., Harding, P., & Schommer, R. 2007, AJ, 133, 290
- Sara, M. M., Bibby, J. L., Zurek, D., et al. 2013, AJ, 146, 162
- Spurzem, R., Berentzen, I., Berczik, P., et al. 2008, The Cambridge *N*-body Lectures, 760, 377
- Spurzem, R. 1999, Journal of Computational and Applied Mathematics, 109, 407
- Spurzem, R., & Aarseth, S. J. 1996, MNRAS, 282, 19
- Stothers, R. B., & Chin, C.-W. 1991, ApJ, 374, 288
- Torres, S., García-Berro, E., Krzesinski, J., & Kleinman, S. J. 2014, A&A, 563, AA47
- Tout, C. A., Aarseth, S. J., Pols, O. R., & Eggleton, P. P. 1997, MNRAS, 291, 732
- Wang, L., Spurzem, R., Aarseth, S.J. et al. 2015, MNRAS, 450, 4070
- Whitmore, B. C., Chandar, R., & Fall, S. M. 2007, AJ, 133, 1067
- Welch, G.A. 1982, ApJ, 259, 77
- van de Ven, G. 2010, IAC Talks, Astronomy and Astrophysics Seminars from the Instituto de Astrofísica de Canarias, 213

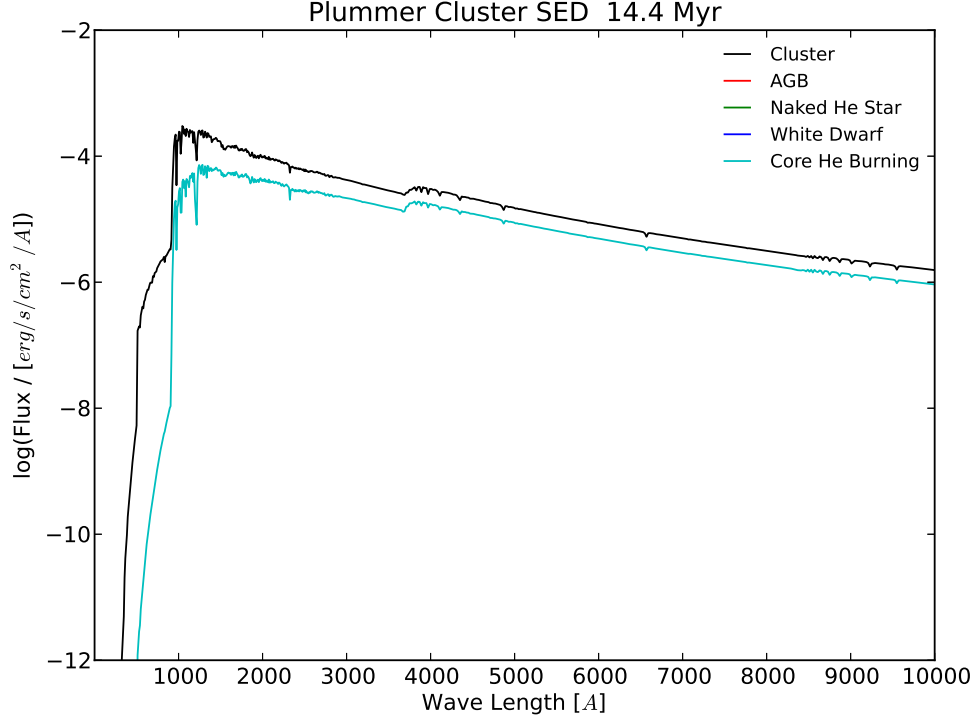


Fig. 1 SED of the simulated cluster (black line) and core helium burning stars (cyan line) at the age of 14.4 Myr. SED of other stellar types will be shown in the following figures. SED of core helium burning stars (stellar type = 4) is indicated as cyan line, AGB stars (stellar type = 5 & 6) red line, naked helium stars (stellar type = 7, 8, 9) green line, white dwarfs (stellar type = 10, 11, 12) blue line. High resolution figures are available for online version.

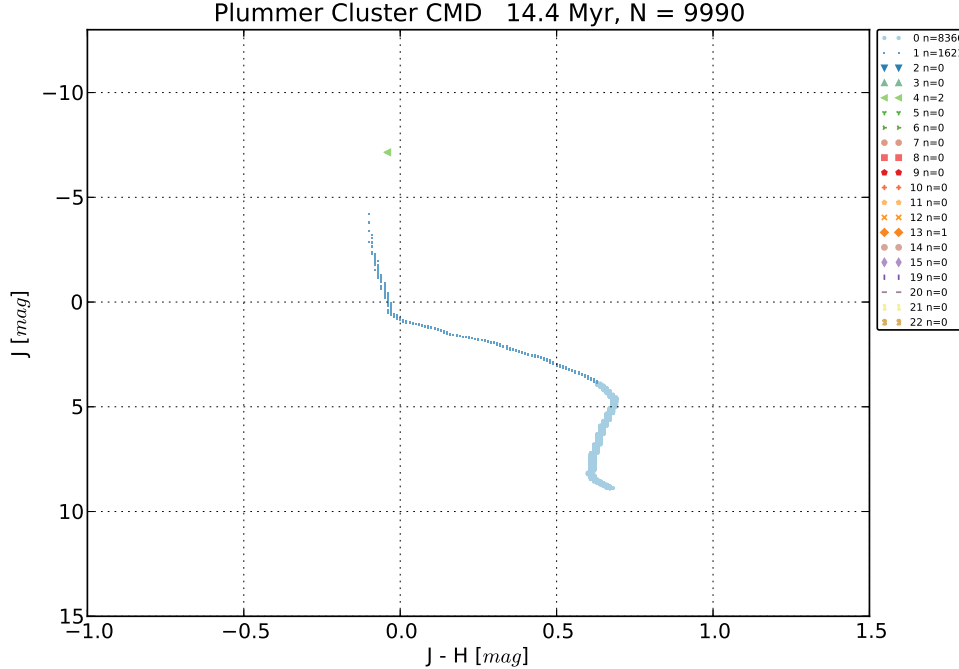


Fig. 2 J-H Color-Magnitude diagram of the simulated cluster at the age of 14.4 Myr. N is the total number of stars, and n is the number of stars of each stellar type indicated in the separate box to the right. Stellar types (see Table 3) are marked with different color and by different symbols. Main sequence stars (Light blue filled round dot: stellar type = 0; sky blue one-pixel point: stellar type = 1) and core helium burning stars (light green left pointing triangle: stellar

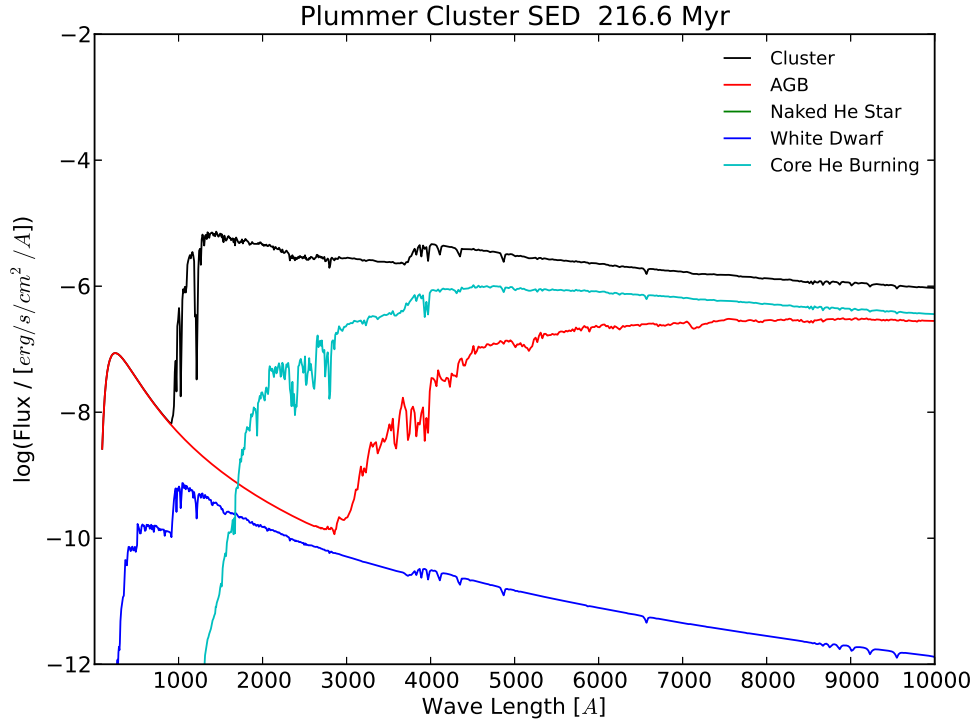


Fig. 3 SED of the simulated cluster (black line), AGB stars (red line), core helium burning stars (cyan line) and white dwarfs (blue line) at the age of 216.6 Myr. Color coding is the same as Figure 1. High resolution figures are available for online version.

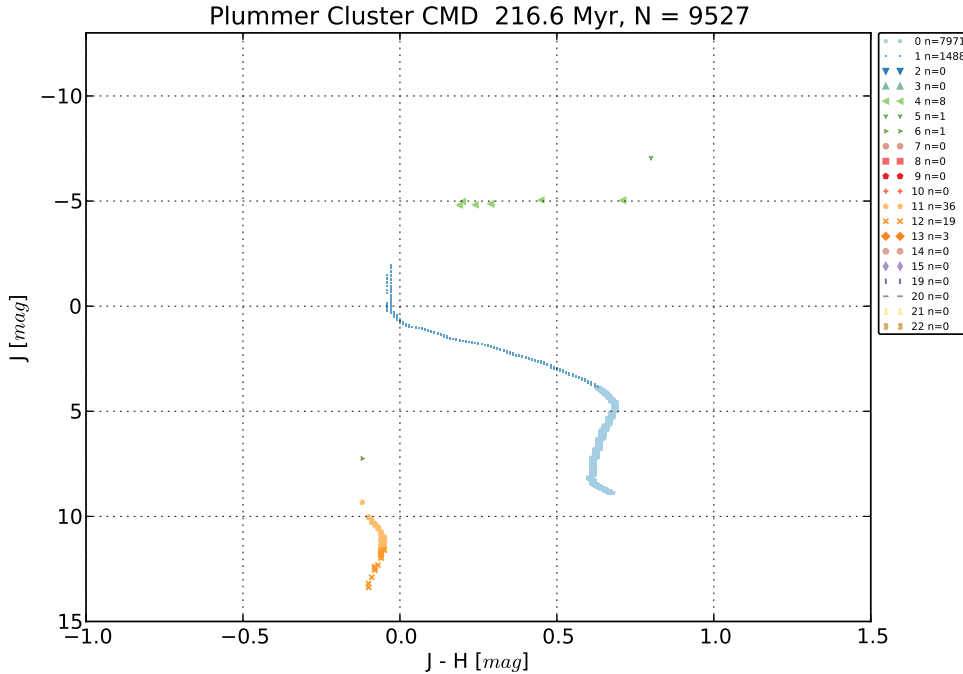


Fig. 4 J-H Color-Magnitude diagram of the simulated cluster at the age of 216.6 Myr. N is the total number of stars, and n is the number of stars of each stellar type indicated in the separate box to the right. Stellar types (see Table 3) are marked with different color and by different symbols. Main sequence stars (Light blue filled round dot: stellar type = 0; sky blue one-pixel point: stellar type = 1), core helium burning stars (light green left-pointing-triangle: stellar type = 4), AGB stars (green downward-tripple-point: stellar type = 5; green upward-tripple-point: stellar type = 6) and white dwarfs (yellow star: stellar type = 11; orange x: cross: stellar type = 12; orange dot: stellar type = 13; orange triangle: stellar type = 14; orange square: stellar type = 15; orange diamond: stellar type = 16; orange circle: stellar type = 17; orange star: stellar type = 18; orange cross: stellar type = 19; orange triangle: stellar type = 20; orange square: stellar type = 21; orange diamond: stellar type = 22).

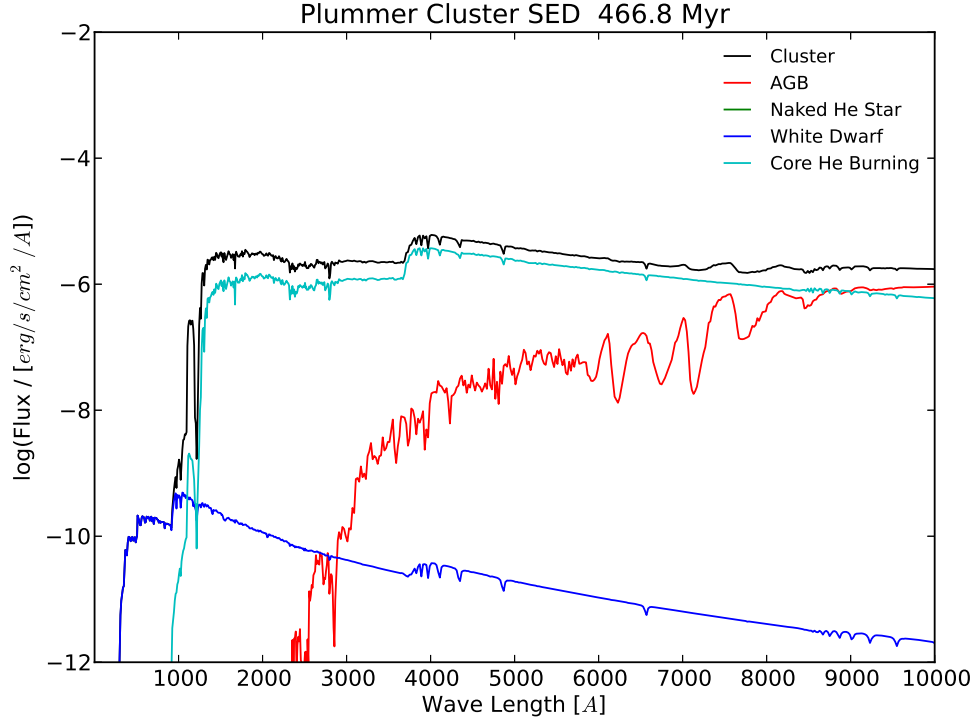


Fig. 5 SED of the simulated cluster (black line), AGB stars (red line), core helium burning stars (cyan line) and white dwarfs (blue line) at the age of 466.8 Myr. Color coding is the same as Figure 1. High resolution figures are available for online version.

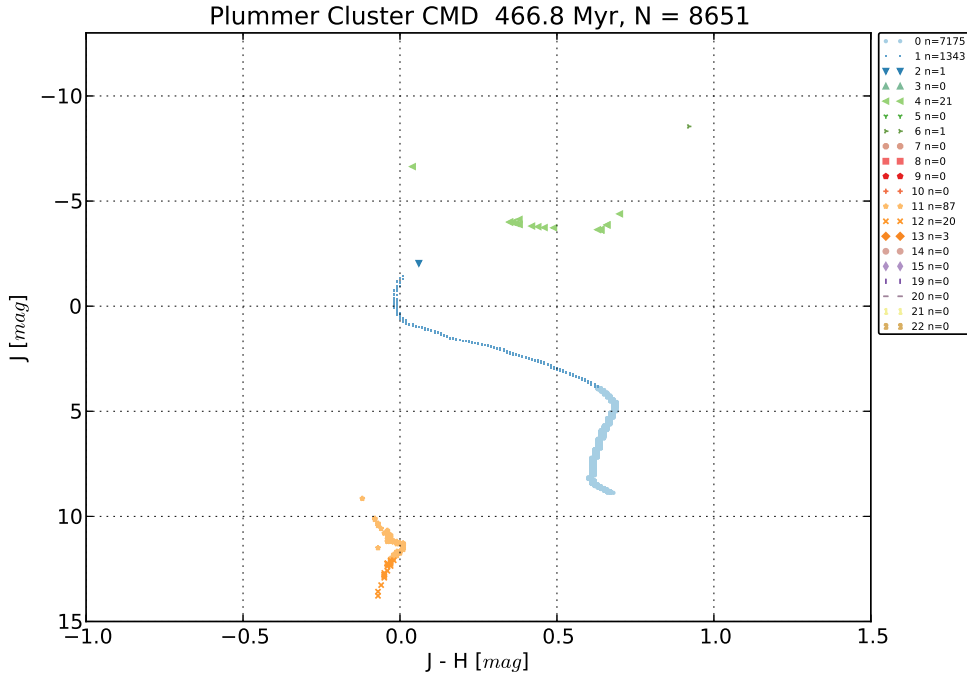


Fig. 6 J-H Color-Magnitude diagram of the simulated cluster at the age of 466.8 Myr. N is the total number of stars, and n is the number of stars of each stellar type indicated in the separate box to the right. Stellar types (see Table 3) are marked with different color and by different symbols. Main sequence stars (Light blue filled round dot: stellar type = 0; sky blue one-pixel point: stellar type = 1), Hertzspung gap stars (dark blue filled downward-triangle: stellar type = 2), core helium burning stars (light green left-pointing-triangle: stellar type = 4), AGB stars (green upward-triangle: stellar type = 6) and white dwarfs (yellow stars: stellar type = 11).

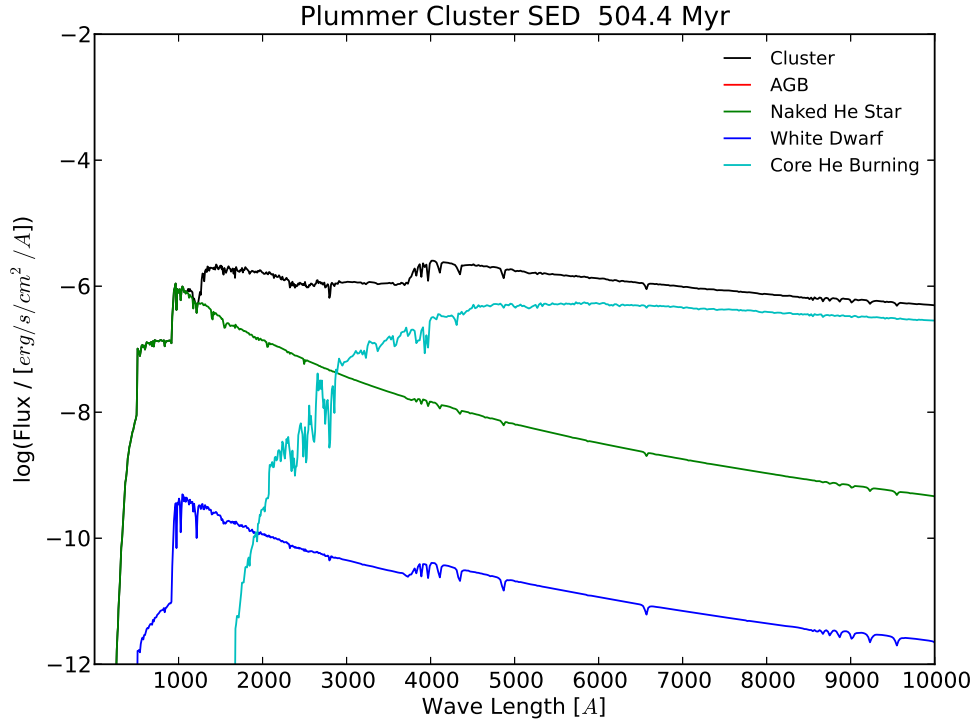


Fig. 7 SED of the simulated cluster (black line) naked helium stars (green line), core helium burning stars (cyan line) and white dwarfs (blue line) at the age of 504.4 Myr. Color coding is the same as Figure 1. High resolution figures are available for online version.

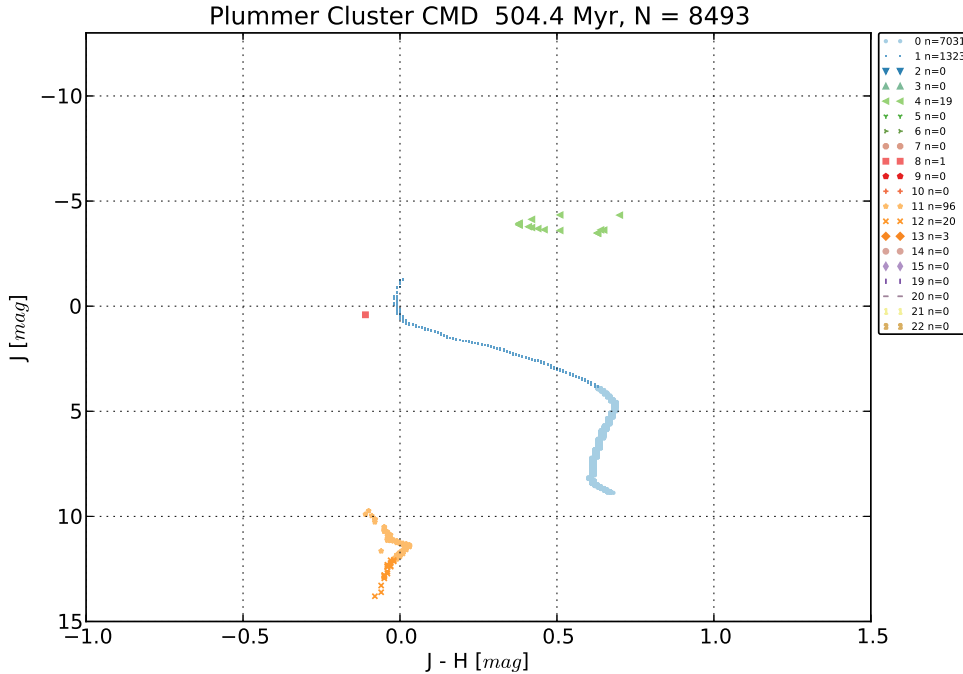


Fig. 8 J-H Color-Magnitude diagram of the simulated cluster at the age of 504.4 Myr. N is the total number of stars, and n is the number of stars of each stellar type indicated in the separate box to the right. Stellar types (see Table 3) are marked with different color and by different symbols. Main sequence stars (Light blue filled round dot: stellar type = 0; sky blue one-pixel point: stellar type = 1), naked helium burning stars (pink-red square: stellar type = 8), core helium burning stars (light green left-pointing-triangle: stellar type = 4), and white dwarfs (yellow star: stellar type = 11; orange x: stellar type = 12) appear in this CMD.